

arXiv:1812.07987v1 [physics.acc-ph] 19 Dec 2018

The Compact Linear e^+e^- Collider (CLIC): Accelerator and Detector

Input to the European Particle Physics Strategy Update
on behalf of the CLIC and CLICdp Collaborations

18 December 2018

Contact person: A. Robson[1)*†]

Editors: P. N. Burrows[*‡], N. Catalan Lasheras[*], L. Linssen[*], M. Petrič[*],
A. Robson[*†], D. Schulte[*], E. Sicking[*], S. Stapnes[*], W. Wuensch[*]

[*] *CERN, Switzerland,* [†] *University of Glasgow, United Kingdom,* [‡] *University of Oxford, United Kingdom*

Abstract

The Compact Linear Collider (CLIC) is a TeV-scale high-luminosity linear e^+e^- collider under development by international collaborations hosted by CERN. This document provides an overview of the design, technology, and implementation aspects of the CLIC accelerator and the detector. For an optimal exploitation of its physics potential, CLIC is foreseen to be built and operated in stages, at centre-of-mass energies of 380 GeV, 1.5 TeV and 3 TeV, for a site length ranging between 11 km and 50 km. CLIC uses a two-beam acceleration scheme, in which normal-conducting high-gradient 12 GHz accelerating structures are powered via a high-current drive beam. For the first stage, an alternative with X-band klystron powering is also considered. CLIC accelerator optimisation, technical developments, and system tests have resulted in significant progress in recent years. Moreover, this has led to an increased energy efficiency and reduced power consumption of around 170 MW for the 380 GeV stage, together with a reduced cost estimate of approximately 6 billion CHF. The detector concept, which matches the physics performance requirements and the CLIC experimental conditions, has been refined using improved software tools for simulation and reconstruction. Significant progress has been made on detector technology developments for the tracking and calorimetry systems. The construction of the first CLIC energy stage could start as early as 2026 and first beams would be available by 2035, marking the beginning of a physics programme spanning 25–30 years and providing excellent sensitivity to Beyond Standard Model physics, through direct searches and via a broad set of precision measurements of Standard Model processes, particularly in the Higgs and top-quark sectors.

© 2022 CERN for the benefit of the CLIC and CLICdp Collaborations.
Reproduction of this article or parts of it is allowed as specified in the CC-BY-4.0 license.

[1] aidan.robson@cern.ch

1. Introduction

The Compact Linear Collider (CLIC) is a multi-TeV high-luminosity linear e^+e^- collider under development by the CLIC accelerator collaboration [1]. It is the only mature multi-TeV lepton collider proposal. CLIC uses a novel two-beam acceleration technique, with normal-conducting accelerating structures operating in the range of 70–100 MV/m. Detailed studies of the physics potential and detector for CLIC, and R&D on detector technologies, are carried out by the CLIC detector and physics (CLICdp) collaboration [1].

The CLIC Conceptual Design Report (CDR) was published in 2012 [2–4]. The main focus of the CDR was to demonstrate the feasibility of the CLIC accelerator at 3 TeV and to confirm that high-precision physics measurements can be performed in the presence of particles from beam-induced background. Following the completion of the CDR, detailed studies on Higgs and top-quark physics, with particular focus on the first energy stage, concluded that the optimal centre-of-mass energy for the CLIC first stage is $\sqrt{s} = 380$ GeV.

As a result, a comprehensive optimisation study of the CLIC accelerator complex was performed, by scanning the full parameter space for the accelerating structures, and by using the luminosity, cost, and energy consumption as a gauge for operation at 380 GeV and 3 TeV. The results led to optimised accelerator design parameters for the proposed staging scenario, with operation at 380 GeV, 1.5 TeV and 3 TeV [5]. The recently updated luminosities for each stage are given in Table 1. CLIC provides $\pm 80\%$ longitudinal electron polarisation and proposes a sharing between the two polarisation states at each energy stage for optimal physics reach [6].

Table 1: Baseline CLIC energy stages and integrated luminosities, $\mathscr{L}_{\text{int}}$, for each stage in the updated scenario [6].

Stage	$\sqrt{s}$ [TeV]	$\mathscr{L}_{\text{int}}$ [ab^{-1}]
1	0.38 (and 0.35)	1.0
2	1.5	2.5
3	3.0	5.0

This document summarises the current progress of the CLIC studies. There have been many recent achievements in accelerator design, technology development, and system tests, described in detail in [7] and summarised in [8]. Large-scale CLIC-specific beam tests have taken place, and crucial experience has been gained from the expanding field of Free Electron Laser (FEL) linacs and new-generation light sources. Together they provide the demonstration that all the CLIC design parameters are well understood and achieved in beam tests, confirming that the performance goals are realistic. An alternative scenario for the first stage, where the accelerating structures are powered by X-band klystrons, has also been studied. The implementation of CLIC at CERN has been investigated, including civil engineering, electrical networks, cooling and ventilation, installation scheduling, transport, and safety aspects. Systematic studies have put emphasis on optimising cost and energy efficiency.

Since the completion of the CDR, the CLIC detector was further optimised through a broad range of simulation studies, resulting in the CLICdet detector design [9, 10]. In order to increase the angular acceptance of the detector, the final focusing quadrupoles are now placed outside the detector in the accelerator tunnel. The software suite for simulation and event reconstruction was modernised and tuned for use with CLICdet. Detector technology developments have focused on the most challenging aspects of the experiment, namely the light-weight silicon vertex and tracker system and the highly-granular calorimeters. The detector R&D activities have resulted in technology demonstrators, showing that the required performance is already achievable or will be achieved in the next phase, compatible with the CLIC timescale [11].

Section 2 provides an overview of the CLIC accelerator design and performance at 380 GeV for both the two-beam baseline design and the klystron-based option. It describes the path to the higher energies, 1.5 TeV and 3 TeV, and gives an overview of the key technology developments. Section 2 also outlines key achievements from beam experiments and hardware tests, providing evidence that the performance goals can be met. The present plans for the CLIC implementation, with emphasis on the 380 GeV stage, are given, as well as estimates of the energy consumption and of the cost for construction and operation. In Section 3 the CLIC detector and its performance results through simulation and event reconstruction are described. Recent progress on detector technology developments is summarised.

CLIC provides excellent sensitivity to Beyond Standard Model physics, through direct searches and via a broad set of precision measurements of Standard Model processes, particularly in the Higgs and top-quark sectors. The physics potential at the three energy stages has been explored in detail [12–14] and is presented in a separate submission to the European Strategy Update process, 'The Compact Linear e^+e^- Collider (CLIC): Physics Potential' [15]; this and supporting documents can be found at the following location:

Supporting documents: `http://clic.cern/european-strategy`

2. CLIC Accelerator

The current staged CLIC design is based on the concepts and R&D results of the CDR [2–4] and on further studies that have since been carried out. The design of the first energy stage, with a luminosity target of $\mathscr{L} = 1.5 \times 10^{34}\,\mathrm{cm}^{-2}\,\mathrm{s}^{-1}$, has been systematically optimised for cost [5]. To limit the cost of the upgrades, the ability to reuse the components in higher-energy stages has been integrated into the design. The parameters for the different energy stages are given in Table 2.

Design and performance at 380 GeV and extension to higher energies A schematic overview of the accelerator configuration for the first energy stage is shown in Figure 1. The main electron beam is produced in a conventional radio frequency (RF) injector, which allows polarisation. The beam emittance is then reduced in a damping ring. To produce the positron beam, an electron beam is accelerated to 5 GeV and sent into a crystal to produce energetic photons, which hit a second target and produce electron–positron pairs. The positrons are captured and accelerated to 2.86 GeV. Their beam emittance is reduced, first in a pre-damping ring and then in a damping ring. The ring to main linac system accelerates both beams to 9 GeV, compresses their bunch length, and delivers the beams to the main linacs. The main linacs accelerate the beams to the collision energy of 190 GeV. The beam delivery system removes transverse tails and off-energy particles with collimators and compresses the beam to the small size required at the interaction point (IP). After collision, the beams are transported by the post collision lines to their respective beam dumps.

To reach multi-TeV collision energies in an acceptable site length and at affordable cost, the main linacs use normal conducting X-band accelerating structures; these achieve a high accelerating gradient of 100 MV/m. For the first energy stage, a lower gradient of 72 MV/m is the optimum to achieve the luminosity goal, which requires a larger beam current than at higher energies.

In order to produce and support high gradients, the accelerating structures are required to be fed by short, very high power RF pulses, which are difficult to generate at acceptable cost and efficiency using conventional klystrons. In order to provide the necessary high peak power, the novel drive-beam scheme uses low-frequency klystrons to efficiently generate long RF pulses and to store their energy in a long, high-current drive-beam pulse. This beam pulse is used to generate many short, even higher intensity pulses that are distributed alongside the main linac, where they release the stored energy in power extraction and transfer structures (PETS) in the form of short RF power pulses, transferred via waveguides into the accelerating structures. This concept strongly reduces the cost and power consumption compared with powering the structures directly by klystrons.

The upgrade to higher energies involves lengthening the main linacs: connecting new tunnels to the existing tunnels, moving the existing modules to the beginning of the new tunnels, and adding new, higher-gradient modules. When upgrading to 1.5 TeV, the length of the beam delivery system (BDS) needs to be increased and new magnets

Table 2: Key parameters of the CLIC energy stages.

Parameter	Symbol	Unit	Stage 1	Stage 2	Stage 3
Centre-of-mass energy	$\sqrt{s}$	GeV	380	1500	3000
Repetition frequency	f_{rep}	Hz	50	50	50
Number of bunches per train	n_{b}		352	312	312
Bunch separation	Δt	ns	0.5	0.5	0.5
Pulse length	τ_{RF}	ns	244	244	244
Accelerating gradient	G	MV/m	72	72/100	72/100
Total luminosity	$\mathscr{L}$	$10^{34}\,\mathrm{cm}^{-2}\,\mathrm{s}^{-1}$	1.5	3.7	5.9
Luminosity above 99% of $\sqrt{s}$	$\mathscr{L}_{0.01}$	$10^{34}\,\mathrm{cm}^{-2}\,\mathrm{s}^{-1}$	0.9	1.4	2
Total integrated luminosity per year	$\mathscr{L}_{\mathrm{int}}$	fb^{-1}	180	444	708
Main linac tunnel length		km	11.4	29.0	50.1
Number of particles per bunch	N	10^9	5.2	3.7	3.7
Bunch length	σ_z	µm	70	44	44
IP beam size	σ_x/σ_y	nm	149/2.9	$\sim$ 60/1.5	$\sim$ 40/1
Normalised emittance (end of linac)	$\varepsilon_x/\varepsilon_y$	nm	900/20	660/20	660/20
Final RMS energy spread		%	0.35	0.35	0.35
Crossing angle (at IP)		mrad	16.5	20	20

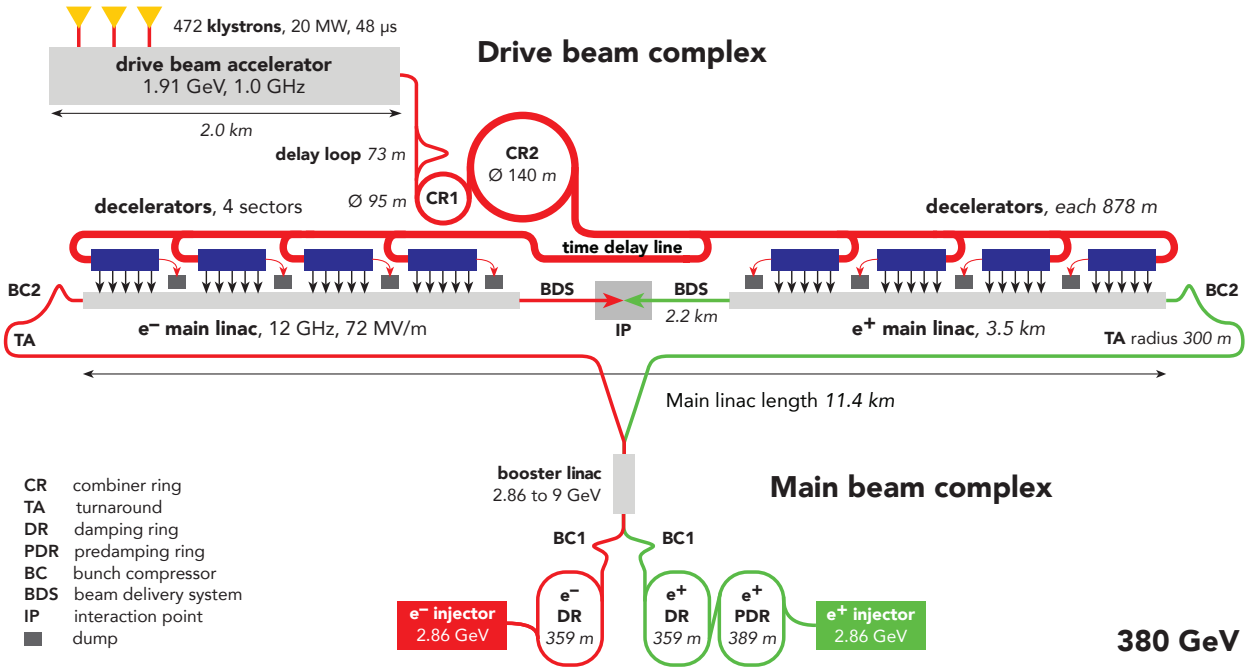
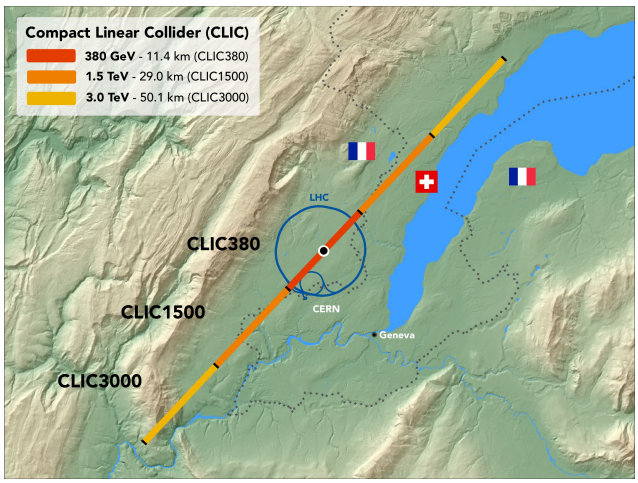


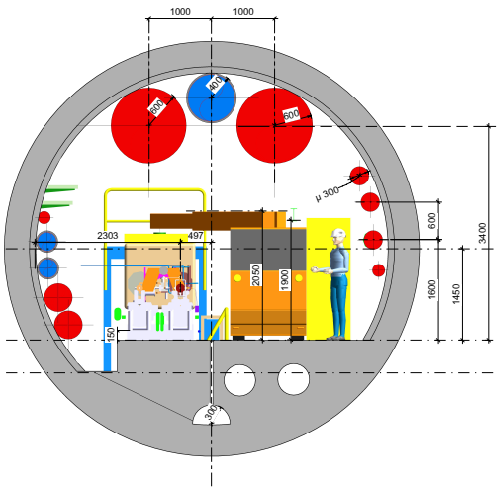
Figure 1: Schematic layout of the CLIC complex at 380 GeV. (image credit: CLIC)

installed. For the BDS upgrade to 3 TeV, only new magnets are required. The central main-beam production complex needs only minor modifications for the first upgrade, to adjust to the smaller number and charge of the bunches, and needs no further modifications for the second upgrade. For the upgrade to 1.5 TeV, the central drive-beam complex needs to be slightly extended to increase the drive-beam energy. For the upgrade to 3 TeV, a second drive-beam complex must be added. This staged collider can be implemented at CERN, as shown in Figure 2(a). The main-beam and drive-beam production facilities are located at the CERN Prévessin site and the tunnel of the first two energy stages would be fully in molasse, which is ideal for tunnelling. The main linac tunnel cross section is shown in Figure 2(b).

The CLIC beam energy can be adjusted to meet different physics requirements. In particular, a period of operation around 350 GeV is foreseen to scan the top-quark pair-production threshold. Operation at much lower energies can also be considered. At the Z-pole, between 2.5 fb^{-1} and 45 fb^{-1} can be achieved per year for an unmodified and a modified collider, respectively.



(a)



(b)

Figure 2: (a) The CLIC main linac footprint near CERN, showing the three implementation stages. (b) The CLIC main linac tunnel cross section for the drive-beam design. (image credit: CLIC)

Klystron-based alternative While the drive-beam scheme is optimal for the high-energy stages, an alternative design for the 380 GeV stage has been considered, in which the main linac accelerating structures are directly powered by klystrons. This increases the cost per GeV in the main linac but it removes the cost of the drive-beam generation complex. This means that it could be a competitive alternative at lower energies provided that the cost of X-band klystrons and their modulators were sufficiently reduced. The klystron-based design is very similar to the drive-beam baseline. It requires a larger main linac tunnel that is separated into two parts by a shielding wall. One part contains the accelerator; the other, the klystrons and related equipment. The collider can be upgraded by extending the main linacs with new sections that are powered by a drive beam.

Performance of the drive-beam concept The focus of accelerating structure development has been on achieving a gradient of 100 MV/m as required for the second and third energy stages. The complex phenomena that occur at such high field levels, especially vacuum breakdown, have been understood, paving the way for the development of an RF design methodology, fabrication techniques, and operational procedures that reduce the breakdown likelihood; the target is to have a rate of less than 3×10^{-7} m^{-1} per beam pulse. This ensures that only 1% of the beam pulses experience a breakdown anywhere along the linacs, even at the 3 TeV stage. Over a dozen prototype accelerating structures, with parameters consistent with beam dynamics requirements, have now been operated at gradients above 100 MV/m for extended periods in dedicated test stands [7]. A summary of the performances achieved in recent tests is shown in Figure 3.

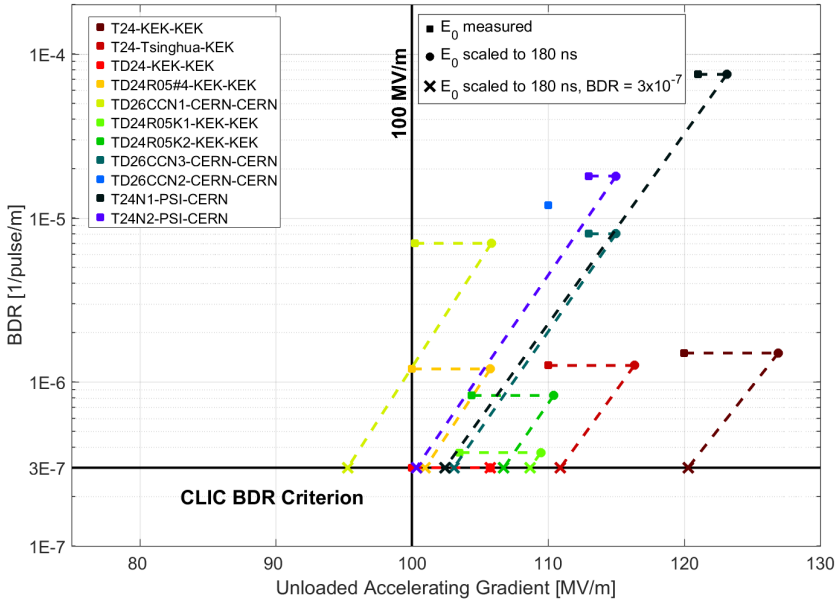


Figure 3: A summary of achieved performances of 3 TeV acceleration structures in tests. The vertical axis represents the breakdown rate (BDR) per metre. The final operating conditions of the tests are indicated by squares. Known scaling is used to determine the performance for the nominal CLIC pulse duration (dashed lines connecting squares to circles) and subsequently for the CLIC-specified breakdown rate of 3×10^{-7} m^{-1} per pulse (dashed lines connecting circles to crosses). Ten prototype structures can be seen operating above the target gradient of 100 MV/m. (image credit: CLIC)

To test the drive-beam concept, the CLIC Test Facility (CTF3) [16] was constructed and operated by an international collaboration. The hardware and experiments addressed the key points of the two-beam concept. This included the demonstration of the high transfer efficiency from the RF to the drive beam and the stable drive-beam acceleration, as well as the generation of the final short, high-current pulse using a delay loop and combiner ring. It also assessed the final beam quality. In particular, feedback was used to stabilise the drive-beam current and phase to ensure correct main-beam acceleration. CTF3 achieved the drive-beam phase stability that is required for CLIC [17–19]. Finally, the drive beam was used to accelerate the main beam with a maximum gradient of 145 MV/m. This established the feasibility of the drive-beam concept and its use to accelerate a main beam.

CTF3 has also been instrumental in developing and testing many different hardware components that are essential for the two-beam acceleration scheme and in validating their performance. Among them are the drive-beam gun, the bunch

compressor, drive-beam accelerating structures, RF deflectors, PETS including a power-off mechanism, the power distribution waveguide system, fast-feedback systems, and drive-beam current and phase monitors. Figure 4 shows the two-beam test stand that integrates all the critical components for the drive-beam deceleration, main-beam acceleration process. CTF3 stopped operation after successfully completing its experimental programme in December 2016 and a new facility, CLEAR, has started to operate. CLEAR re-uses the CTF3 main-beam installations and additional hardware for further beam dynamics studies, with a focus on the main beam.

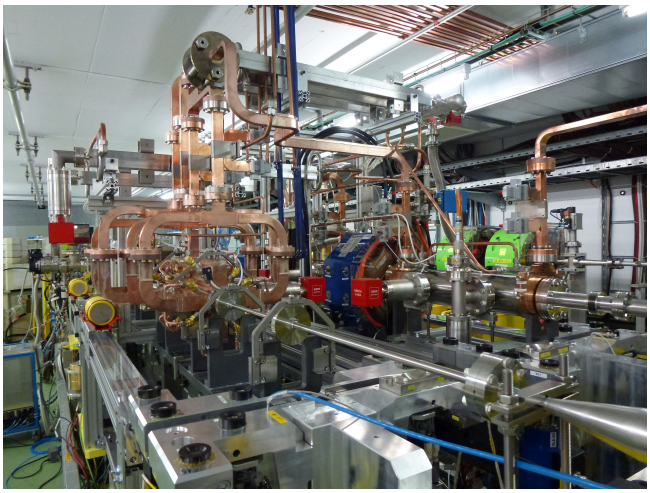


Figure 4: The two-beam acceleration test stand in the CTF3 facility. The drive beam enters from the middle-right, while the probe (main) beam enters from the bottom-right. (image credit: CLIC)

Luminosity performance The baseline plan for operating CLIC includes a yearly shutdown of 120 days, 30 days of commissioning, 20 days for machine development, and 10 days for planned technical stops. This leaves 185 days of operation for collider physics data-taking. Assuming an availability during normal running of 75%, this results in an integrated luminosity per year equivalent to operating at full luminosity for 1.2×10^7 s [20].

In order to achieve high luminosity, CLIC requires very small beam sizes at the collision point, as listed in Table 2. The resulting high charge density leads to strong beam–beam effects, which result in the emission of beamstrahlung and production of background particles. This is limited to an acceptable level by using flat beams, which are much larger in the horizontal than in the vertical plane. The key to high luminosity lies in the small vertical beam size, and therefore a small vertical emittance and strong vertical focusing are essential.

The vertical emittance and consequently the luminosity are to a large extent determined by imperfections in the accelerator complex; without them a luminosity of $\mathscr{L} = 4.3 \times 10^{34}\,\mathrm{cm}^{-2}\,\mathrm{s}^{-1}$ would be reached at $\sqrt{s} = 380\,\mathrm{GeV}$. The nominal luminosity of $\mathscr{L} = 1.5 \times 10^{34}\,\mathrm{cm}^{-2}\,\mathrm{s}^{-1}$ takes into account the impact of the different imperfections; significant margin has been added to the known effects to enhance the robustness of the design. Important examples of imperfections are the misalignment of components after the installation and the vibrations of the quadrupoles due to ground motion.

Novel system designs and technologies in combination with beam-based tuning minimise the effect of imperfections, and simulated performances provide full luminosity at the 3 TeV stage. While this is not strictly necessary for the initial energy stage, where the performance specifications could be relaxed, this choice avoids the need for these systems to be upgraded for the higher-energy stages. Key technologies that have been developed include the pre-alignment and quadrupole stabilisation systems as well as high-precision beam instrumentation. Pre-alignment at the 10 µm-level is required for the main linac and BDS components. An active alignment system achieves this, using actuators and sensors to remotely align the 2 m-long modules that support the main linac components with respect to a stretched-wire reference network. The alignment system has been successfully tested. The disks that make up the accelerating structures are fabricated in industry to micron tolerance and are bonded together to a tolerance of ten microns. To mitigate the effect of wakefields caused by misalignments, the accelerating structures are equipped with monitors that measure this wakefield to determine the offset of the structure from the beam. The remote alignment system uses this information to minimise the wakefield effects on the beam. A nm-level vibration stabilisation system for both main linac and final focus quadrupoles, which is based on actuators and inertial sensors, allows decoupling of the focusing magnets from the ground. This is important to avoid the natural ground motion as well as vibrations induced by technical equipment that could lead to beam jitter and reduced luminosity. Ground motion has been measured at CERN, and CLIC is designed to withstand the noise that has been measured in the CMS detector cavern. Other key technologies that have been developed include hybrid, high-gradient final quadrupoles, and advanced wigglers for the damping rings.

In addition to the hardware tests, beam experiments provide the evidence that CLIC can reach its performance goals. The Swiss Light Source and the Australian Light Source have reached CLIC-level vertical emittances [21, 22]. The advanced beam-based alignment of the CLIC main linac has successfully been tested in FACET and FERMI [23, 24].

Other technology developments Further technology developments include the main linac modules and their auxiliary sub-systems such as vacuum, stable supports, and instrumentation. Many developments have focused primarily on cost and power reduction [7]. In both the drive-beam and klystron-based versions of CLIC, all of the power going to the

beam flows through klystrons. Their efficiency is thus crucial to the overall efficiency of the facility. Recently, new klystron beam dynamics concepts have been established, in studies driven by the CLIC collaboration, which result in significant efficiency increases over a broad range of frequencies and power levels. The concepts have been successfully demonstrated in a test of a retrofitted S-band klystron. The concepts are now being implemented in both the L-band drive-beam klystrons and in the X-band main linac klystron designs for CLIC, as well as klystrons for other projects that require high RF production efficiency. CLIC requires several thousand focusing quadrupoles in the drive beam. Adjustable permanent magnet prototypes have been developed that reduce the power needs as well as the power supply and cabling costs.

Beam instrumentation, including sub-micron level resolution beam-position monitors with time accuracy better than 20 ns and bunch-length monitors with resolution better than 20 fs, have been developed and tested with beam in CTF3. CLIC technology developments have also had a strong influence on small-scale, compact accelerator applications from many fields. The modularity of CLIC has the consequence that much of the linac technology, especially that relating to high-gradient acceleration, is directly relevant for photon sources, medical linacs and beam manipulation devices. The adoption of CLIC technology for these applications is now providing a significant boost to CLIC, especially through an enlarging commercial supplier base [25].

Construction, cost estimate, and power consumption The technology and construction-driven timeline for the CLIC programme is given in Figure 5 [7]. This schedule has seven years of initial construction and commissioning, potentially starting in 2026. Including a two-year margin this leads to first collisions in 2035. The 27 years of CLIC data-taking include two intervals of two years between the stages.

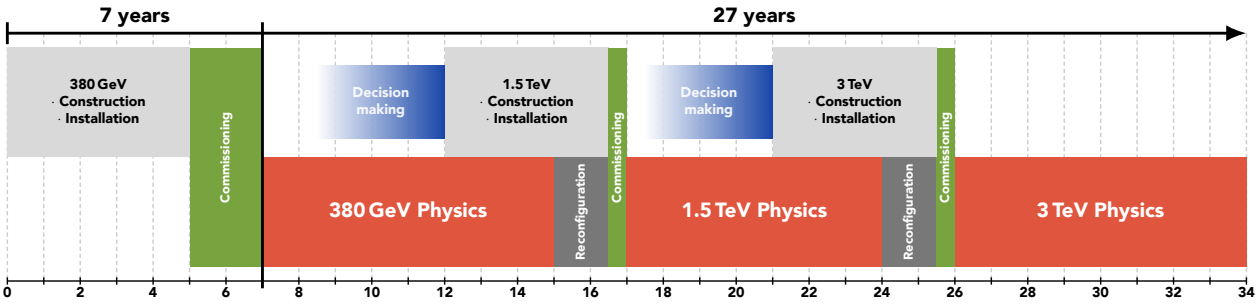


Figure 5: Technology and construction-driven CLIC schedule, showing the construction and commissioning period and the three stages for data taking. The time needed for reconfiguration (connection, hardware commissioning) between the stages is also indicated. (image credit: CLIC)

The cost estimate of the initial stage is approximately 5.9 billion CHF. The energy upgrade to 1.5 TeV has an estimated cost of approximately 5.1 billion CHF, including the upgrade of the drive-beam RF power. The cost of the further energy upgrade to 3 TeV has been estimated at approximately 7.3 billion CHF, including the construction of a second drive-beam complex.

The nominal power consumption at the 380 GeV stage is approximately 170 MW. Recent power savings at the 380 GeV stage have not yet been scrutinised for the 1.5 TeV and 3 TeV stages, but earlier estimates give approximately 370 MW and 590 MW, respectively [2]. The annual energy consumption for nominal running at the initial energy stage is estimated to be 0.8 TWh. For comparison, CERN's current energy consumption is approximately 1.2 TWh per year, of which the accelerator complex uses approximately 90%.

Further details on the schedule, cost estimate, and power consumption, including for the klystron-based option, are given in the Addendum and in [7].

3. CLIC detector design, technologies and performance

The CLIC detector is a general-purpose detector designed to provide excellent performance for known e^+e^- physics processes as well as being prepared for a broad range of potential Beyond Standard Model (BSM) signatures. Its design and technology choices are driven by the CLIC physics objectives and the experimental conditions. In this section, the requirements and design of the CLIC detector are summarised, followed by a description of the detector technology choices and the status of the detector R&D. Examples of the detector performance are also given.

In view of the physics objectives, the required track momentum resolution is $\sigma_{p_T}/p_T^2 \leq 2\times10^{-5}\,\mathrm{GeV}^{-1}$ for high-energy charged particles in the central detector region, needed e.g. for the precision measurement of heavy states decaying into leptons. For optimal flavour tagging a resolution of 5 µm in the transverse impact parameter, d_0, is required for single tracks in the central detector that have p_T above a few GeV. The corresponding limit on material thickness is $0.2\%\,X_0$ per layer in the vertex detector and $2\%\,X_0$ per layer in the tracker. A single hit position resolution of 3 µm is required in the vertex detector and 7 µm in the tracker. The jet energy resolution, σ_E/E, is required to be better than 5% for light-quark jets of 50 GeV, and better than 3.5% for jet energies above 100 GeV. This is needed, for example, to separate W, Z and H hadronic decays. Accurate jet reconstruction through particle flow analysis (PFA) is at the origin of the choice of highly-granular sampling calorimetry. Detector coverage for electrons and photons is needed down to small polar angles and 10 mrad is targeted.

As shown in Table 2, beams at CLIC arrive in bunch trains of 156–176 ns duration. During each bunch train at most one hard e^+e^- collision is expected, while background particles from beamstrahlung will be spread in time along the bunch train. The low event rates and the CLIC time structure allow for triggerless readout of full bunch trains (at 50 Hz). It also allows the on-detector power to be turned off during the inter-train periods (power pulsing), thereby reducing the cooling needs. Beam-induced backgrounds increase strongly with centre-of-mass energy, and so operation at 3 TeV can be considered the most challenging case for CLIC. The presence of beam-induced backgrounds imposes a hit time resolution of 1 ns in the calorimeters and 5 ns in the tracking system. The design of the CLIC detector foresees small readout cells in order to limit occupancies to at most 3% integrated over the bunch train. This leads to a maximum cell size of $25\times25\,\mu\mathrm{m}^2$ in the vertex detector and maximum cell sizes of 0.05–0.5 mm^2 in the silicon tracker. The small readout cells in the calorimeters will allow not only for accurate jet reconstruction through PFA, but will also provide an indispensable means of recognising particles from beam-induced background through PFA reconstruction, and rejecting those particles by applying cuts on their p_T and arrival time. Except for the very forward regions, radiation levels at CLIC are a factor of about $\sim10^{-4}$ lower than at LHC.

The CLIC detector A view of the CLIC detector (CLICdet) is shown in Figure 6(a). It comprises a low-mass silicon-pixel vertex detector with three double layers in the central barrel and three double layers of forward petals in a spiral arrangement optimised for air cooling. It is surrounded by a 4.5 m long, 1.5 m diameter, low-mass silicon tracker, and highly-granular calorimetry. The silicon tracker has six barrel and seven disk layers for a total surface of 140 m^2. The electromagnetic calorimeter is composed of a 40-layer sandwich with $5\times5\,\mathrm{mm}^2$ silicon pad sensors interspersed with 1.9 mm tungsten plates, for a total depth of $22\,X_0$. The hadronic calorimeter comprises 60 layers of plastic scintillator tiles interspersed with 19 mm thick steel plates, for a total depth of $7.5\,\lambda_I$. The scintillator tiles have $3\times3\,\mathrm{cm}^2$ lateral size and are read out individually by silicon photomultipliers (SiPM). The above detectors are surrounded by a superconducting solenoid providing a magnetic field of 4 T. Detectors for muon identification are inserted into slots in the iron yoke. The forward calorimeters, LumiCal and BeamCal, are optimised for the luminosity measurements and forward-electron tagging. The estimated data volume per bunch train is ∼115 MB at 3 TeV and ∼75 MB at 380 GeV. A more detailed description of CLICdet can be found in [9, 10]. CLICdet was optimised for operation at $\sqrt{s}=3$ TeV. Since background rates at $\sqrt{s}=380$ GeV are lower, some modifications to the inner detector layers are anticipated for the first energy stage [3]. An enlarged view of the vertex detector is shown in Figure 6(b). The forward region of the detector is presented in Figure 6(c).

A significant change with respect to the CDR detector models [3] is the location of the final focusing quadrupole QD0. In order to enlarge the angular coverage of HCAL, QD0 is now located outside of the detector in the accelerator tunnel.

Detector technologies A broad detector technology R&D programme for CLIC is ongoing [11]. In view of the time scales involved and limited resources, the development targets primarily those areas where CLIC requirements are the most challenging: the silicon vertex and tracking system, the high-granularity ECAL and HCAL calorimeter systems, and the forward electromagnetic calorimeters LumiCal and BeamCal.

While the individual performance requirements for the vertex detector can be met using state-of-the art silicon /

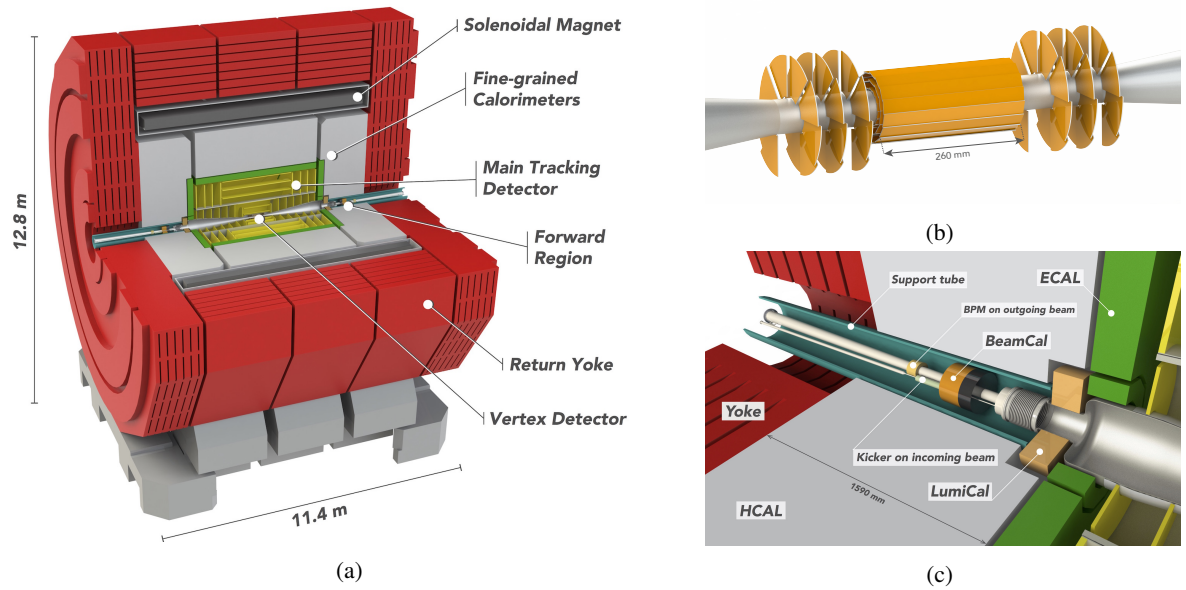


Figure 6: (a) View of CLICdet. (b) View of the vertex detector layout, showing also the spiralling arrangement of the forward petals to facilitate air cooling. (c) Layout of the forward region of CLICdet. (image credit: CLICdp)

CMOS detector technologies, the combination of all requirements is challenging and calls for new technological solutions. The ongoing comprehensive R&D programme involves simulations, readout ASIC and sensor designs, the construction and readout of small detector assemblies, laboratory tests and beam tests. Both hybrid assemblies and depleted monolithic sensors are under study. While the R&D programme focused initially on the vertex detector with small pixels of $25 \times 25\,\mu\text{m}^2$, some of the technologies are now also under consideration for the CLIC tracker.

Given the results of the CLIC silicon vertex and tracker R&D, together with expected advances in semiconductor technologies worldwide, it can be expected that CLIC objectives will be achieved in a timely manner. The following conclusions can be drawn from the results already obtained from the CLIC vertex and tracker R&D [11]:

- Good signal-to-noise ratios have been achieved for the detection of signals from thin (50 µm) fully-depleted planar sensors, sufficient for full detection efficiency and for satisfying the CLIC hit-time requirements.
- For planar sensors, small sensor thicknesses, needed to reach the low-mass requirements, go together with small charge sharing, limiting the achievable position resolution. Sensor designs with enhanced charge sharing are underway and more advanced ASIC process technologies (e.g. 28 nm instead of 65 nm) offer prospects for smaller pixel sizes and better position resolution.
- Promising results were obtained from tests using monolithic CMOS technologies (SOI, HV-CMOS, HR-CMOS). CLIC-specific fully integrated designs are underway. Monolithic technologies offer a potential for high-precision performance over large surfaces, with a reduced material budget and at a lower cost.
- Feasibility of power pulsing was demonstrated for module-size low-mass powering demonstrators, including tests in a magnetic field. Power pulsing was also implemented successfully in hybrid ASICs and HV-CMOS sensors for CLIC. Power consumption levels below $50\,\text{mW}/\text{cm}^2$ have been achieved.
- Feasibility of air cooling was confirmed in a full-scale CLIC vertex detector mock-up with realistic heat loads.

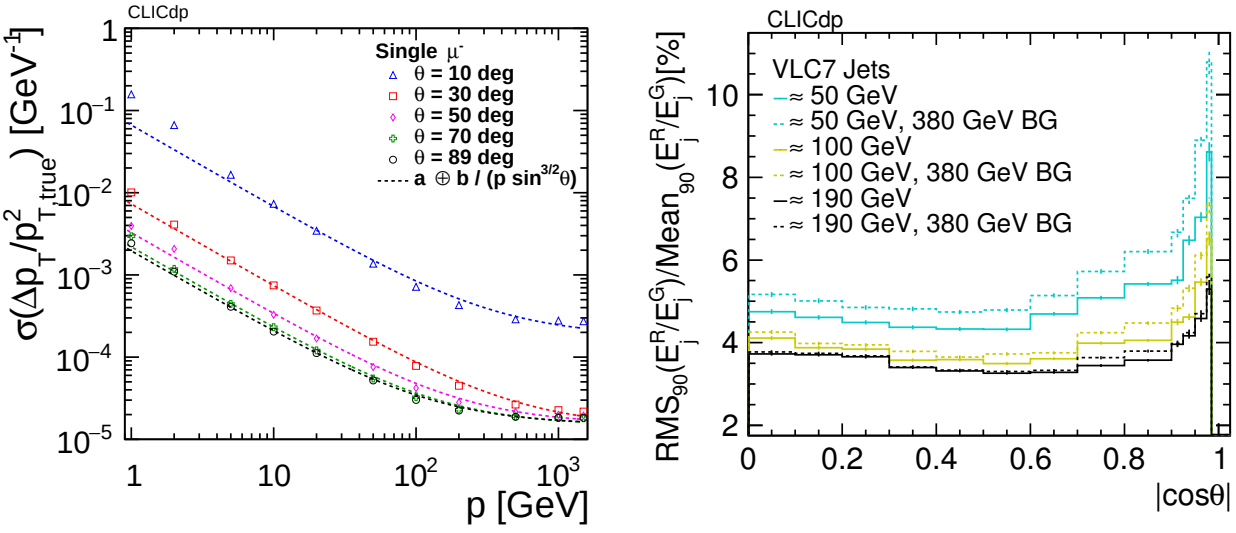
A broad R&D programme towards fine-grained calorimetry technologies is carried out in the framework of the CALICE and FCAL collaborations, in close cooperation with CLICdp. CALICE silicon-tungsten technology R&D for ECAL and scintillator-steel technology R&D with SiPM readout for HCAL proceeded by first building 'physics prototypes'. These devices include the core technology features and are large enough to assess their response to showers from individual particles and to provide detailed shower data for validating the expected CLICdet jet performance through PFA event reconstruction. For the 30-layer SiW ECAL the results show an energy resolution for electrons and photons at the level of $16.6\%/\sqrt{E}$ with a constant term of 1.1%. A 38-layer AHCAL prototype with ~ 7600 readout cells was the first device to use SiPMs on a large scale. Its imaging capabilities allowed the exploitation of shower substructures, such as using MIP tracklets for calibration purposes or using knowledge of local hit density for improving the energy resolution through software compensation. Exposure to 10–80 GeV pions yields an energy resolution at the level of $57.6\%/\sqrt{E}$ with a constant term of 1.6%. This result is further improved to $44.3\%/\sqrt{E}$ with a constant term of 1.8% through software compensation.

The next generation of highly-granular calorimeter prototypes are so-called 'technological prototypes'. Their design includes engineering constraints and scalability features for the construction, which will also be needed for the final detectors. One example is the SiPM-on-tile hadronic calorimeter prototype, comprising 38 detection layers for a total of nearly 22000 scintillator tiles. For this prototype, construction and quality assurance processes have been optimised and automated. Likewise, recent prototypes of the SiW ECAL integrate more of the engineering and scalability aspects, which will be needed for an ECAL system with tens of millions of channels.

Technology development for the compact fine-grained forward electromagnetic calorimeters LumiCal and BeamCal is pursued by the FCAL collaboration. These detectors require a very small Molière radius ($\sim$1 cm) and a very large dynamic range. To this end 4- and 8-layer LumiCal prototypes were constructed and tested. A small effective Molière radius of (8.1 ± 0.3) mm was measured using electron beams of 5 GeV. Due to the large out-of-time beam-induced backgrounds in the forward region, the forward calorimeters are exposed to high radiation levels, e.g. an ionising dose of 1 MGy per year for BeamCal. Therefore, beyond overall detector design, BeamCal technology development is concentrating on radiation-hardness studies of sensor materials (GaAs, sapphire, SiC and silicon diode sensors), and is yielding promising results.

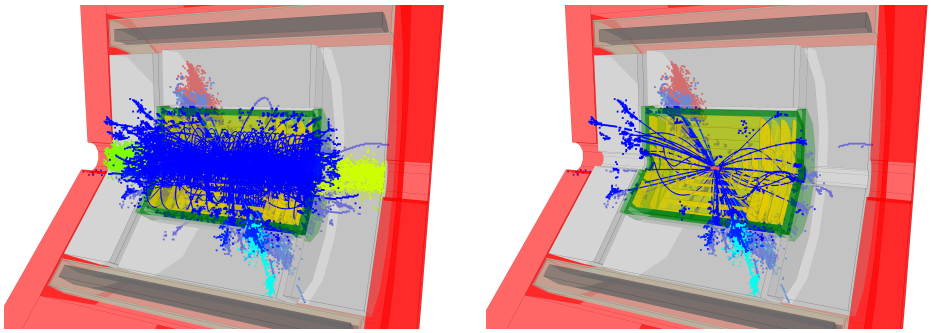
Detector performance The CLICdet performance has been studied through simulation and event reconstruction for single particles, complex events, and jets [10]. To this end the detailed detector geometry has been implemented in the simulation framework; events are generated, and the resulting particles tracked through the detector. For example, Figure 7(a) shows that the transverse momentum resolution requirement is met for high-momentum tracks in the central detector region. The jet energy resolution is presented in Figure 7(b), showing results both for the case without background and for the case with $\sqrt{s} = 380$ GeV equivalent beam-induced background overlaid and subsequently suppressed through the timing cuts mentioned above. More examples can be found in [10], showing that the proposed CLICdet design globally meets the CLIC performance requirements.

To illustrate the effect of the suppression of particles from beam-induced backgrounds, Figure 8 depicts an event display of $e^+e^- \to t\bar{t}$ at $\sqrt{s} = 3$ TeV before and after background suppression using p_T and timing cuts. It shows that beam-induced background particles can be removed efficiently from the event and that the resulting data show a clean boosted back-to-back $e^+e^- \to t\bar{t}$ topology.



(a) (b)

Figure 7: (a) Transverse momentum resolution as a function of momentum for muons at polar angles $\theta = 10^\circ, 30^\circ, 50^\circ, 70^\circ$ and 89°. The lines represent the fit of each curve with the parameterisation as inserted in the figure. (b) Jet energy resolution for various jet energies as a function of $|\cos\theta|$ of the quark with and without 380 GeV $\gamma\gamma \to$ hadrons background overlaid on the physics di-jet event. RMS90 is used as a measure of the jet energy resolution. (image credit: CLICdp)



(a) (b)

Figure 8: $e^+e^- \to t\bar{t}$ event display at a centre-of-mass energy of 3 TeV (a) before, and (b) after background suppression using p_T and timing cuts. (image credit: CLICdp)

4. Summary and Outlook

CLIC is a mature proposal for the next generation of high-energy collider. The choice of $\sqrt{s} = 380\,\text{GeV}$ for the initial-stage energy has been optimised for maximal physics reach, and in turn the accelerator parameters have been systematically optimised for performance at the initial stage, while integrating the energy upgrade plans to 1.5 TeV and 3 TeV into the design. Beam experiments and hardware tests have demonstrated that the CLIC performance goals can be met. For instance, accelerating gradients of up to 145 MV/m have been reached with the two-beam concept at CTF3, and breakdown rates of the accelerating structures well below the limit of $3 \times 10^7\,\text{m}^{-1}$ per beam pulse are being stably achieved at X-band test platforms. Substantial progress has been made towards realising the nanometre-sized beams required by CLIC for high luminosities: the low emittances needed for the CLIC damping rings are achieved by modern synchrotron light sources; special alignment procedures for the main linac are now available; and sub-nanometre stabilisation of the final focus quadrupoles has been demonstrated. Recent developments have resulted in an improved energy efficiency of the 380 GeV stage, with a reduced power consumption of around 170 MW, together with a lower estimated cost, now around 6 billion CHF. The proposed site, at CERN, is well understood.

The project implementation for CLIC foresees a five-year preparation phase prior to construction, which is envisaged to start by 2026. The preparation phase will focus on further design optimisation, technical and industrial development of critical parts of the CLIC accelerator, and further cost and power reduction leading to a TDR around 2025. System verification in FEL linacs and low emittance rings will be increasingly important for the CLIC accelerator performance studies. Furthermore, civil engineering and infrastructure preparation will become progressively more detailed, in parallel with an environmental impact study. The increasing use of X-band technology, either as the main RF technology or for parts of the accelerator, in e.g. compact test-facilities [26], light-sources [27], medical accelerators, or for low-energy particle physics studies [28], provides new collaborative opportunities towards a TDR for the CLIC accelerator.

CLIC detector simulation studies have led to a new, optimised CLIC detector concept, CLICdet. CLICdet is optimised for particle flow with a light-weight vertex and tracking system, highly-granular calorimeter systems, a 4 T solenoid and muon detectors, and very forward calorimeters for luminosity measurements and electron tagging. Detector R&D activities have validated technology demonstrators for vertex and tracking detectors and calorimetry, including the power pulsing of sub-detectors, and cooling concepts optimised for very thin readout layers. For a construction start by 2026, the scope of the detector activities will need to increase significantly in order to cover all detectors, systems and infrastructures. Beyond the present technology demonstrators, full prototypes of all sub-detectors, including the superconducting magnet, will be aimed for. Detector engineering and integration aspects will be worked out in full.

The physics potential of CLIC has been assessed through many new studies and is described in a separate submission [15]. CLIC provides excellent sensitivity to Beyond Standard Model physics, through direct searches and via a broad set of precision measurements of Standard Model processes, particularly in the Higgs and top-quark sectors, which reach well beyond the projections for HL-LHC. Physics studies will continue during the preparation phase, while the development of software tools will remain in pace with the needs of the project. Accordingly, the CLICdp collaboration is expected to develop significantly in size and formal structure. The current CLIC scenario spans 25–30 years of data-taking. Longer-term, novel accelerator technologies [29] can potentially lead to much higher-energy beams. The CLIC installations at CERN could become the home of even higher-energy e^+e^- accelerators after completion of the CLIC programme. Given its mature technical feasibility, outstanding physics reach, and possibility for future expansion, CLIC represents a compelling opportunity for the post-LHC era.

References

[1] *Compact Linear Collider (CLIC)*, last accessed 14 Dec 2018, URL: http://clic.cern/.

[2] M. Aicheler et al., eds.,
A Multi-TeV Linear Collider Based on CLIC Technology: CLIC Conceptual Design Report, CERN-2012-007, 2012, DOI: 10.5170/CERN-2012-007.

[3] L. Linssen et al., eds., *CLIC Conceptual Design Report: Physics and Detectors at CLIC*, CERN-2012-003, 2012, DOI: 10.5170/CERN-2012-003.

[4] P. Lebrun et al., eds., *CLIC Conceptual Design Report: The CLIC Programme: Towards a Staged e^+e^- Linear Collider Exploring the Terascale*, CERN-2012-005, 2012, DOI: 10.5170/CERN-2012-005.

[5] P. N. Burrows et al., eds., *Updated baseline for a staged Compact Linear Collider*, CERN-2016-004, 2016, DOI: 10.5170/CERN-2016-004.

[6] P. Roloff, A. Robson, *Updated CLIC luminosity staging baseline and Higgs coupling prospects*, CLICdp-Note-2018-002, 2018, URL: https://cds.cern.ch/record/2645352.

[7] P. N. Burrows et al., eds., *CLIC Project Implementation Plan*, CERN, 2018,
URL: https://edms.cern.ch/document/2053292/.

[8] P. N. Burrows et al., eds., *The Compact Linear Collider (CLIC) 2018 Summary Report*, CERN-2018-005-M, 2018, DOI: 10.23731/CYRM-2018-002.

[9] N. Alipour Tehrani et al., *CLICdet: The post-CDR CLIC detector model*, CLICdp-Note-2017-001, 2017,
URL: https://cds.cern.ch/record/2254048.

[10] D. Arominski et al., *A detector for CLIC: main parameters and performance*, CLICdp-Note-2018-005, 2018,
URL: http://cds.cern.ch/record/2649437.

[11] D. Dannheim et al., eds., *Detector Technologies for CLIC*, CERN, 2018,
URL: https://edms.cern.ch/document/2053288/.

[12] H. Abramowicz et al., CLICdp Collaboration, *Higgs physics at the CLIC electron-position linear collier*, Eur. Phys. J. **C77** (2017) 475, DOI: 10.1140/epjc/s10052-017-4968-5.

[13] H. Abramowicz et al., CLICdp Collaboration, *Top-Quark Physics at the CLIC Electron-Positron Linear Collider* (2018), arXiv: 1807.02441 [hep-ex].

[14] J. De Blas et al., eds., *The CLIC Potential for New Physics*, CERN, 2018,
URL: https://arxiv.org/abs/1812.02093.

[15] P. Roloff et al., eds., *The Compact Linear e^+e^- Collider (CLIC): Physics Potential*, 2018,
URL: https://cds.cern.ch/record/2652257.

[16] G. Geschonke, A. Ghigo, *CTF3 Design Report*, CERN-PS-2002-008-RF, Geneva, Switzerland, 2002,
URL: https://cds.cern.ch/record/559331.

[17] D. Schulte, R. Tomas, *Dynamic Effects in the New CLIC Main Linac*,
Proceedings of PAC 2009, Vancouver, Canada, 2009, p. 3811,
URL: http://accelconf.web.cern.ch/accelconf/PAC2009/papers/th6pfp046.pdf.

[18] C. Gohil, P. N. Burrows, D. Schulte, *Integrated Simulation of Dynamic Effects for the 380 GeV CLIC Design*, CLIC-Note-1138, 2018, URL: https://cds.cern.ch/record/2649487.

[19] J. Roberts et al., *Stabilization of the arrival time of a relativistic electron beam to the 50 fs level*,
Phys. Rev. Accel. Beams **21** (2018) 011001, DOI: 10.1103/PhysRevAccelBeams.21.011001.

[20] F. Bordry et al.,
Machine Parameters and Projected Luminosity Performance of Proposed Future Colliders at CERN (2018), arXiv: 1810.13022 [physics.acc-ph].

[21] M. Aiba et al., *Ultra low vertical emittance at SLS through systematic and random optimization*,
Nucl. Instrum. Meth. **A694** (2012) 133, DOI: 10.1016/j.nima.2012.08.012.

[22] K. P. Wootton, M. J. Boland, R. P. Rassool,
Measurement of ultralow vertical emittance using a calibrated vertical undulator,
Phys. Rev. ST Accel. Beams **17** (11 2014) 112802, DOI: 10.1103/PhysRevSTAB.17.112802.

[23] *FACET Facility for Advanced Accelerator Experimental Tests*, last accessed 14 Dec 2018, URL:
http://portal.slac.stanford.edu/sites/ard_public/facet/Pages/default.aspx.

[24] *FERMI Free Electron laser Radiation for Multidisciplinary Investigations*, last accessed 14 Dec 2018, URL: https://www.elettra.trieste.it/lightsources/fermi.html.

[25] G. D'Auria et al., *X-band Technology for FEL Sources*, Proceedings of LINAC 2014, Geneva, Switzerland, 2014, MOPP023, URL: http://cds.cern.ch/record/2062591.

[26] M. Diomede et al., *RF Design of the X-band Linac for the EuPRAXIA@SPARC_LAB Project*, Proceedings of IPAC 2018, Vancouver, BC Canada, 2018, p. 4422, DOI: 10.18429/JACoW-IPAC2018-THPMK058.

[27] *CompactLight project*, last accessed 14 Dec 2018, URL: http://www.compactlight.eu/.

[28] T. Akesson et al., *Dark Sector Physics with a Primary Electron Beam Facility at CERN*, CERN-SPSC-2018-023, SPSC-EOI-018, Geneva, 2018, URL: http://cds.cern.ch/record/2640784.

[29] B. Cros, P. Muggli, eds., *Towards a Proposal for an Advanced Linear Collider, Report on the Advanced and Novel Accelerators for High Energy Physics Roadmap Workshop*, 2017, URL: https://cds.cern.ch/record/2298632.

[30] D. Dannheim et al., *Cost estimate for CLICdet*, LCD-Note-2018-005, 2018, URL: https://edms.cern.ch/document/2027873/.

A. Addendum

Appendix A.1 lists the CLIC scientific community, Appendix A.2 gives further details on the timeline, Appendix A.3 gives further details on the construction and operating costs, and Appendix A.4 gives a short discussion of the computing requirements.

A.1. Community

The CLIC accelerator collaboration and CLIC Detector and Physics collaboration together comprise around 400 participants from approximately 75 institutes worldwide [1]. Additional contributions are made from beyond the collaborations. This report is submitted on behalf of the authors of the Compact Linear Collider (CLIC) 2018 Summary Report [8]:

T.K. Charles, P.J. Giansiracusa, T.G. Lucas, R.P. Rassool, M. Volpi[1]
University of Melbourne, Melbourne, Australia

C. Balazs
Monash University, Melbourne, Australia

K. Afanaciev, V. Makarenko
Belarusian State University, Minsk, Belarus

A. Patapenka, I. Zhuk
Joint Institute for Power and Nuclear Research - Sosny, Minsk, Belarus

C. Collette
Université libre de Bruxelles, Brussels, Belgium

M.J. Boland
University of Saskatchewan, Saskatoon, Canada

A.C. Abusleme Hoffman, M.A. Diaz, F. Garay
Pontificia Universidad Católica de Chile, Santiago, Chile

Y. Chi, X. He, G. Pei, S. Pei, G. Shu, X. Wang, J. Zhang, F. Zhao, Z. Zhou
Institute of High Energy Physics, Beijing, China

H. Chen, Y. Gao, W. Huang, Y.P. Kuang, B. Li, Y. Li, X. Meng, J. Shao, J. Shi, C. Tang, P. Wang, X. Wu, H. Zha
Tsinghua University, Beijing, China

L. Ma, Y. Han
Shandong University, Jinan, China

W. Fang, Q. Gu, D. Huang, X. Huang, J. Tan, Z. Wang, Z. Zhao
Shanghai Institute of Applied Physics, Chinese Academy of Sciences, Shanghai, China

U.I. Uggerhøj, T.N. Wistisen
Aarhus University, Aarhus, Denmark

A. Aabloo, R. Aare, K. Kuppart, S. Vigonski, V. Zadin
University of Tartu, Tartu, Estonia

M. Aicheler, E. Baibuz, E. Brücken, F. Djurabekova[2], P. Eerola[2], F. Garcia, E. Haeggström[2], K. Huitu[2], V. Jansson[2], I. Kassamakov[2], J. Kimari[2], A. Kyritsakis, S. Lehti, A. Meriläinen[2], R. Montonen[2], K. Nordlund[2], K. Österberg[2], A. Saressalo, J. Väinölä, M. Veske
Helsinki Institute of Physics, University of Helsinki, Helsinki, Finland

W. Farabolini, A. Mollard, F. Peauger[3], J. Plouin
CEA, Gif-sur-Yvette, France

P. Bambade, I. Chaikovska, R. Chehab, N. Delerue, M. Davier, A. Faus-Golfe, A. Irles, W. Kaabi, F. LeDiberder, R. Pöschl, D. Zerwas
Laboratoire de l'Accélérateur Linéaire, Université de Paris-Sud XI, IN2P3/CNRS, Orsay, France

B. Aimard, G. Balik, J.-J. Blaising, L. Brunetti, M. Chefdeville, A. Dominjon, C. Drancourt, N. Geoffroy, J. Jacquemier, A. Jeremie, Y. Karyotakis, J.M. Nappa, M. Serluca, S. Vilalte, G. Vouters
LAPP, Université de Savoie, IN2P3/CNRS, Annecy, France

A. Bernhard, E. Bründermann, S. Casalbuoni, S. Hillenbrand, J. Gethmann, A. Grau, E. Huttel, A.-S. Müller, P. Peiffer[4], I. Perić, D. Saez de Jauregui
Karlsruhe Institute of Technology (KIT), Karlsruhe, Germany

L. Emberger, C. Graf, F. Simon, M. Szalay, N. van der Kolk[5]
Max-Planck-Institut für Physik, Munich, Germany

S. Brass, W. Kilian
Department of Physics, University of Siegen, Siegen, Germany

T. Alexopoulos, T. Apostolopoulos[6], E.N. Gazis, N. Gazis, V. Kostopoulos[7], S. Kourkoulis
National Technical University of Athens, Athens, Greece

B. Heilig
Department of Basic Geophysical Research, Mining and Geological Survey of Hungary, Tihany, Hungary

J. Lichtenberger
Space Research Laboratory, Eötvös Loránd University, Budapest, Hungary

P. Shrivastava
Raja Ramanna Centre for Advanced Technology, Department of Atomic Energy, Indore, India

M.K. Dayyani, H. Ghasem[1], S.S. Hajari, H. Shaker[1]
The School of Particles and Accelerators, Institute for Research in Fundamental Sciences, Tehran, Iran

Y. Ashkenazy, I. Popov, E. Engelberg, A. Yashar
Racah Institute of Physics, Hebrew University of Jerusalem, Jerusalem, Israel

H. Abramowicz, Y. Benhammou, O. Borysov, M. Borysova, A. Levy, I. Levy
Raymond & Beverly Sackler School of Physics & Astronomy, Tel Aviv University, Tel Aviv, Israel

D. Alesini, M. Bellaveglia, B. Buonomo, A. Cardelli, M. Diomede, M. Ferrario, A. Gallo, A. Ghigo, A. Giribono, L. Piersanti, A. Stella, C. Vaccarezza
INFN e Laboratori Nazionali di Frascati, Frascati, Italy

J. de Blas
Università di Padova and INFN, Padova, Italy

R. Franceschini
Università degli Studi Roma Tre and INFN, Roma, Italy

G. D'Auria, S. Di Mitri
Elettra Sincrotrone Trieste, Trieste, Italy

T. Abe, A. Aryshev, M. Fukuda, K. Furukawa, H. Hayano, Y. Higashi, T. Higo, K. Kubo, S. Kuroda, S. Matsumoto, S. Michizono, T. Naito, T. Okugi, T. Shidara, T. Tauchi, N. Terunuma, J. Urakawa, A. Yamamoto[1]
High Energy Accelerator Research Organization, KEK, Tsukuba, Japan

R. Raboanary
University of Antananarivo, Antananarivo, Madagascar

O.J. Luiten, X.F.D. Stragier
Eindhoven University of Technology, Eindhoven, Netherlands

R. Hart, H. van der Graaf
Nikhef, Amsterdam, Netherlands

G. Eigen
Department of Physics and Technology, University of Bergen, Bergen, Norway

E. Adli[1], C.A. Lindstrøm, R. Lillestøl, L. Malina[1], J. Pfingstner, K.N. Sjobak[1]
University of Oslo, Oslo, Norway

A. Ahmad, H. Hoorani, W.A. Khan
National Centre for Physics, Islamabad, Pakistan

S. Bugiel, R. Bugiel, M. Firlej, T.A. Fiutowski, M. Idzik, J. Moroń, K.P. Świentek
AGH University of Science and Technology, Krakow, Poland

P. Brückman de Renstrom, B. Krupa, M. Kucharczyk, T. Lesiak, B. Pawlik, P. Sopicki, B. Turbiarz, T. Wojtoń, L.K. Zawiejski
Institute of Nuclear Physics, Polish Academy of Sciences, Krakow, Poland

J. Kalinowski, K. Nowak, A.F. Żarnecki
Faculty of Physics, University of Warsaw, Warsaw, Poland

E. Firu, V. Ghenescu, A.T. Neagu, T. Preda, I. S. Zgura
Institute of Space Science, Bucharest, Romania

A. Aloev, N. Azaryan, I. Boyko, J. Budagov, M. Chizhov, M. Filippova, V. Glagolev, A. Gongadze, S. Grigoryan, D. Gudkov, V. Karjavine, M. Lyablin, Yu. Nefedov, A. Olyunin[1], A. Rymbekova, A. Samochkine, A. Sapronov, G. Shelkov, G. Shirkov, V. Soldatov, E. Solodko[1], G. Trubnikov, I. Tyapkin, V. Uzhinsky, A. Vorozhtov, A. Zhemchugov
Joint Institute for Nuclear Research, Dubna, Russia

E. Levichev, N. Mezentsev, P. Piminov, D. Shatilov, P. Vobly, K. Zolotarev
Budker Institute of Nuclear Physics, Novosibirsk, Russia

I. Božović Jelisavčić, G. Kačarević, G. Milutinović Dumbelović, M. Pandurović, M. Radulović, J. Stevanović, N. Vukasinović
Vinča Institute of Nuclear Sciences, University of Belgrade, Belgrade, Serbia

D.-H. Lee
School of Space Research, Kyung Hee University, Yongin, Gyeonggi, South Korea

N. Ayala, G. Benedetti, T. Guenzel, U. Iriso, Z. Marti, F. Perez, M. Pont
CELLS-ALBA, Barcelona, Spain

J. Trenado
University of Barcelona, Barcelona, Spain

A. Ruiz-Jimeno, I. Vila
IFCA, CSIC-Universidad de Cantabria, Santander, Spain

J. Calero, M. Dominguez, L. Garcia-Tabares, D. Gavela, D. Lopez, F. Toral
Centro de Investigaciones Energéticas, Medioambientales y Tecnológicas (CIEMAT), Madrid, Spain

C. Blanch Gutierrez, M. Boronat, D. Esperante[1], E. Fullana, J. Fuster, I. García, B. Gimeno, P. Gomis Lopez, D. González, M. Perelló, E. Ros, M.A. Villarejo, A. Vnuchenko, M. Vos
Instituto de Física Corpuscular (CSIC-UV), Valencia, Spain

R. Brenner, Ch. Borgmann, T. Ekelöf, M. Jacewicz, M. Olvegård, R. Ruber, V. Ziemann
Uppsala University, Uppsala, Sweden

D. Aguglia, J. Alabau Gonzalvo, M. Alcaide Leon, N. Alipour Tehrani, M. Anastasopoulos, A. Andersson, F. Andrianala[8], F. Antoniou, A. Apyan, D. Arominski[9], K. Artoos, S. Assly, S. Atieh, C. Baccigalupi, R. Ballabriga Sune, D. Banon Caballero, M.J. Barnes, J. Barranco Garcia, A. Bartalesi, J. Bauche, C. Bayar, C. Belver-Aguilar, A. Benot Morell[10], M. Bernardini, D.R. Bett, S. Bettoni[11], M. Bettencourt, B. Bielawski, O. Blanco Garcia, N. Blaskovic Kraljevic, B. Bolzon[12], X.A. Bonnin, D. Bozzini, E. Branger, E. Brondolin, O. Brunner, M. Buckland[13], H. Bursali, H. Burkhardt, D. Caiazza, S. Calatroni, M. Campbell, N. Catalan Lasheras, B. Cassany, E. Castro, R.H. Cavaleiro Soares, M. Cerqueira Bastos, A. Cherif, E. Chevallay, V. Cilento[14], R. Corsini, R. Costa[15], B. Cure, S. Curt, A. Dal Gobbo, D. Dannheim, E. Daskalaki, L. Deacon, A. Degiovanni, G. De Michele, L. De Oliveira, V. Del Pozo Romano, J.P. Delahaye, D. Delikaris, P.G. Dias de Almeida[16], T. Dobers, S. Doebert, I. Doytchinov, M. Draper, F. Duarte Ramos, M. Duquenne, N. Egidos Plaja, K. Elsener, J. Esberg, M. Esposito, L. Evans, V. Fedosseev, P. Ferracin, A. Fiergolski, K. Foraz, A. Fowler, F. Friebel, J-F. Fuchs, A. Gaddi, D. Gamba, L. Garcia Fajardo[17], H. Garcia Morales, C. Garion, M. Gasior, L. Gatignon, J-C. Gayde, A. Gerbershagen, H. Gerwig, G. Giambelli, A. Gilardi, A.N. Goldblatt, S. Gonzalez Anton, C. Grefe[18], A. Grudiev, H. Guerin, F.G. Guillot-Vignot, M.L. Gutt-Mostowy, M. Hein Lutz, C. Hessler, J.K. Holma, E.B. Holzer, M. Hourican, D. Hynds[19], E. Ikarios, Y. Inntjore Levinsen, S. Janssens, A. Jeff, E. Jensen, M. Jonker, S.W. Kamugasa, M. Kastriotou, J.M.K. Kemppinen, V. Khan, R.B. Kieffer, W. Klempt, N. Kokkinis, I. Kossyvakis, Z. Kostka, A. Korsback, E. Koukovini Platia, J.W. Kovermann, C-I. Kozsar, I. Kremastiotis[20], J. Kröger[21], S. Kulis, A. Latina, F. Leaux, P. Lebrun, T. Lefevre, E. Leogrande, L. Linssen, X. Liu, X. Llopart Cudie, S. Magnoni, C. Maidana, A.A. Maier, H. Mainaud Durand, S. Mallows, E. Manosperti, C. Marelli, E. Marin Lacoma, S. Marsh, R. Martin, I. Martini, M. Martyanov, S. Mazzoni, G. Mcmonagle, L.M. Mether, C. Meynier, M. Modena, A. Moilanen, R. Mondello, P.B. Moniz Cabral, N. Mouriz Irazabal, M. Munker, T. Muranaka, J. Nadenau, J.G. Navarro, J.L. Navarro Quirante, E. Nebo Del Busto, N. Nikiforou[22], P. Ninin, M. Nonis, D. Nisbet, F.X. Nuiry, A. Nürnberg[23], J. Ögren, J. Osborne, A.C. Ouniche, R. Pan[24], S. Papadopoulou, Y. Papaphilippou, G. Paraskaki, A. Pastushenko[10], A. Passarelli, M. Patecki, L. Pazdera, D. Pellegrini, K. Pepitone, E. Perez Codina, A. Perez Fontenla, T.H.B. Persson, M. Petrič[25], S. Pitman, F. Pitters[26], S. Pittet, F. Plassard, D. Popescu, T. Quast[27], R. Rajamak, S. Redford[11], L. Remandet, Y. Renier[24], S.F. Rey, O. Rey Orozco, G. Riddone, E. Rodriguez Castro, P. Roloff, C. Rossi, F. Rossi, V. Rude, I. Ruehl, G. Rumolo, A. Sailer, J. Sandomierski, E. Santin, C. Sanz, J. Sauza Bedolla, U. Schnoor, H. Schmickler, D. Schulte, E. Senes, C. Serpico, G. Severino, N. Shipman, E. Sicking, R. Simoniello[28], P.K. Skowronski, P. Sobrino Mompean, L. Soby, P. Sollander, A. Solodko, M.P. Sosin, S. Spannagel, S. Sroka, S. Stapnes, G. Sterbini, G. Stern, R. Ström, M.J. Stuart, I. Syratchev, K. Szypula, F. Tecker, P.A. Thonet, P. Thrane, L. Timeo, M. Tiirakari, R. Tomas Garcia, C.I. Tomoiaga, P. Valerio[29], T. Vaňát, A.L. Vamvakas, J. Van Hoorne, O. Viazlo, M. Vicente Barreto Pinto[30], N. Vitoratou, V. Vlachakis, M.A. Weber, R. Wegner, M. Wendt, M. Widorski, O.E. Williams, M. Williams[31], B. Woolley, W. Wuensch, A. Wulzer, J. Uythoven, A. Xydou, R. Yang, A. Zelios, Y. Zhao[32], P. Zisopoulos
CERN, Geneva, Switzerland

M. Benoit, D M S Sultan
Département de Physique Nucléaire et Corpusculaire (DPNC), Université de Genève, Genève, Switzerland

F. Riva[1]
Département de Physique Théorique, Université de Genève, Genève, Switzerland

M. Bopp, H.H. Braun, P. Craievich, M. Dehler, T. Garvey, M. Pedrozzi, J.Y. Raguin, L. Rivkin[33], R. Zennaro
Paul Scherrer Institut, Villigen, Switzerland

S. Guillaume, M. Rothacher
ETH Zurich, Institute of Geodesy and Photogrammetry, Zurich, Switzerland

A. Aksoy, Z. Nergiz[34], Ö. Yavas
Ankara University, Ankara, Turkey

H. Denizli, U. Keskin, K. Y. Oyulmaz, A. Senol
Department of Physics, Abant İzzet Baysal University, Bolu, Turkey

A.K. Ciftci
Izmir University of Economics, Izmir, Turkey

V. Baturin, O. Karpenko, R. Kholodov, O. Lebed, S. Lebedynskyi, S. Mordyk, I. Musienko, Ia. Profatilova, V. Storizhko
Institute of Applied Physics, National Academy of Sciences of Ukraine, Sumy, Ukraine

R.R. Bosley, T. Price, M.F. Watson, N.K. Watson, A.G. Winter
University of Birmingham, Birmingham, United Kingdom

J. Goldstein
University of Bristol, Bristol, United Kingdom

S. Green, J.S. Marshall[35], M.A. Thomson, B. Xu, T. You[36]
Cavendish Laboratory, University of Cambridge, Cambridge, United Kingdom

W.A. Gillespie
University of Dundee, Dundee, United Kingdom

M. Spannowsky
Department of Physics, Durham University, Durham, United Kingdom

C. Beggan
British Geological Survey, Edinburgh, United Kingdom

V. Martin, Y. Zhang
University of Edinburgh, Edinburgh, United Kingdom

D. Protopopescu, A. Robson[1]
University of Glasgow, Glasgow, United Kingdom

R.J. Apsimon[37], I. Bailey[38], G.C. Burt[37], A.C. Dexter[37], A.V. Edwards[37], V. Hill[37], S. Jamison, W.L. Millar[37], K. Papke[37]
Lancaster University, Lancaster, United Kingdom

G. Casse, J. Vossebeld
University of Liverpool, Liverpool, United Kingdom

T. Aumeyr, M. Bergamaschi[1], L. Bobb[38], A. Bosco, S. Boogert, G. Boorman, F. Cullinan, S. Gibson, P. Karataev, K. Kruchinin, K. Lekomtsev, A. Lyapin, L. Nevay, W. Shields, J. Snuverink, J. Towler, E. Yamakawa
The John Adams Institute for Accelerator Science, Royal Holloway, University of London, Egham, United Kingdom

V. Boisvert, S. West
Royal Holloway, University of London, Egham, United Kingdom

R. Jones, N. Joshi
University of Manchester, Manchester, United Kingdom

D. Bett, R.M. Bodenstein[1], T. Bromwich, P.N. Burrows[1], G.B. Christian[38], C. Gohil[1], P. Korysko[1], J. Paszkiewicz[1], C. Perry, R. Ramjiawan, J. Roberts
John Adams Institute, Department of Physics, University of Oxford, Oxford, United Kingdom

T. Coates, F. Salvatore
University of Sussex, Brighton, United Kingdom

A. Bainbridge[37], J.A. Clarke[37], N. Krumpa, B.J.A. Shepherd[37], D. Walsh[3]
STFC Daresbury Laboratory, Warrington, United Kingdom

S. Chekanov, M. Demarteau, W. Gai, W. Liu, J. Metcalfe, J. Power, J. Repond, H. Weerts, L. Xia, J. Zhang
Argonne National Laboratory, Argonne, USA

J. Zupan
Department of Physics, University of Cincinnati, Cincinnati, OH, USA

J.D. Wells, Z. Zhang
Physics Department, University of Michigan, Ann Arbor, MI, USA

C. Adolphsen, T. Barklow, V. Dolgashev, M. Franzi, N. Graf, J. Hewett, M. Kemp, O. Kononenko, T. Markiewicz, K. Moffeit, J. Neilson, Y. Nosochkov, M. Oriunno, N. Phinney, T. Rizzo, S. Tantawi, J. Wang, B. Weatherford, G. White, M. Woodley
SLAC National Accelerator Laboratory, Menlo Park, USA

[1]Also at CERN, Geneva, Switzerland
[2]Also at Department of Physics, University of Helsinki, Helsinki, Finland
[3]Now at CERN, Geneva, Switzerland
[4]Now at Johannes-Gutenberg University, Mainz, Germany
[5]Now at Nikhef / Utrecht University, Amsterdam / Utrecht, The Netherlands
[6]Also at Department of Informatics, Athens University of Business and Economics, Athens, Greece
[7]Also at University of Patras, Patras, Greece
[8]Also at University of Antananarivo, Antananarivo, Madagascar
[9]Also at Warsaw University of Technology, Warsaw, Poland
[10]Also at IFIC, Valencia, Spain
[11]Now at Paul Scherrer Institute, Villigen, Switzerland
[12]Now at CEA, Gif-sur-Yvette, France
[13]Also at University of Liverpool, United Kingdom
[14]Also at LAL, Orsay, France
[15]Also at Uppsala University, Uppsala, Sweden
[16]Also at IFCA, CSIC-Universidad de Cantabria, Santander, Spain
[17]Now at LBNL, Berkeley CA, USA
[18]Now at University of Bonn, Bonn, Germany
[19]Now at Nikhef, Amsterdam, The Netherlands
[20]Also at KIT, Karlsruhe, Germany
[21]Also at Ruprecht-Karls-Universität Heidelberg, Germany
[22]Now at University of Texas, Austin, USA
[23]Now at Karlsruhe Institute of Technology, Karlsruhe, Germany
[24]Now at DESY, Zeuthen, Germany
[25]Also at J. Stefan Institute, Ljubljana, Slovenia
[26]Also at Vienna University of Technology, Vienna, Austria
[27]Also at RWTH Aachen University, Aachen, Germany
[28]Now at Johannes Gutenberg Universität, Mainz, Germany
[29]Now at Département de Physique Nucléaire et Corpusculaire (DPNC), Université de Genève, Geneva, Switzerland
[30]Also at Département de Physique Nucléaire et Corpusculaire (DPNC), Université de Genève, Geneva, Switzerland
[31]Also at University of Glasgow, Glasgow, United Kingdom
[32]Also at Shandong University, Jinan, China
[33]Also at EPFL, Lausanne, Switzerland
[34]Also at Omer Halis Demir University, Nigde, Turkey
[35]Now at University of Warwick, Coventry, United Kingdom
[36]Also at DAMTP, University of Cambridge, Cambridge, United Kingdom
[37]Also at The Cockcroft Institute, Daresbury, United Kingdom
[38]Now at Diamond Light Source, Harwell, United Kingdom

A.2. Schedule

The construction schedules are based on the same methodologies used for the CLIC CDR [2]. Details about the various parameters used can be found in [7]. The construction, installation, and commissioning schedule for the 380 GeV drive-beam design is shown in Figure 9 and lasts for 7 years. It comprises:

- Slightly more than five years for the excavation and tunnel lining, the installation of the tunnel infrastructures, and the accelerator equipment transport and installation.
- Eight months for the system commissioning, followed by two months for final alignment.
- One year for the accelerator commissioning with beam.

In parallel, time and resources are allocated for the construction of the drive-beam surface building, the combiner rings, damping rings, main-beam building and experimental areas, and their corresponding system installation and commissioning, as shown in Figure 9.

In the klystron-based 380 GeV option, the time needed for construction, installation and commissioning is 8 years.

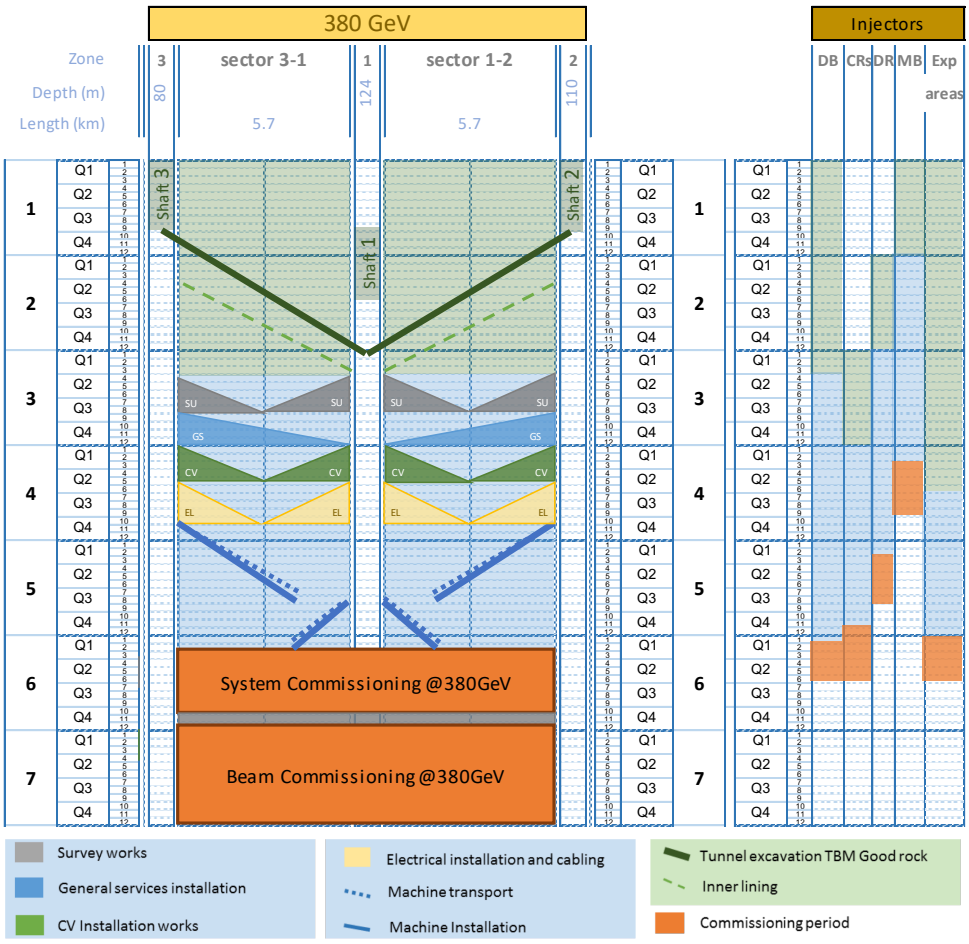


Figure 9: Construction and commissioning schedule for the 380 GeV drive-beam based CLIC facility. The vertical axis represents time in years. The abbreviations are introduced in Figure 1. (image credit: CLIC)

The 380 GeV collider is designed to be extended to higher energies. Most of the construction and installation work can be carried out in parallel with the data-taking. However, it is estimated that a stop of two years in accelerator operation is needed between two energy stages. This time is needed to make the connection between the existing machine and its extensions, to reconfigure the modules used at the existing stage for their use at the next stage, to modify the beam-delivery system, to commission the new equipment, and to commission the entire new accelerator complex with beam.

In a schedule driven by technology and construction, the CLIC project would cover 34 years, counted from the start of construction: around 7 years for construction and commissioning and a total of 27 years for data-taking at the three energy stages, including two 2-year intervals between the stages.

A.3. Costings and power consumption

Construction costs The initial energy stage of CLIC has been fully re-costed in 2018, using the same method as previous CLIC cost estimates and those of other projects such as the LHC experiments and the Reference Design Report and Technical Design Report of the International Linear Collider (ILC). Since the CLIC CDR, many CLIC optimisation studies have been undertaken with a particular focus on cost reduction. Further details of the cost estimate are given in [8] and full details in [7]; only a brief summary is given here. For the cost estimate, CLIC is assumed to be a CERN-hosted project, constructed and operated within a collaborative framework with participation and contributions from many international partners. A "value and explicit labour" methodology is applied, and for the value estimates a bottom-up approach is used that follows the work breakdown structure of the project. Estimates are given for both the drive-beam based and klystron-based options. The uncertainty objective for the final outcome is $\pm 25\%$. Uncertainties on individual items are grouped into two categories: *technical uncertainty*, relating to technological maturity and likelihood of evolution in design or configuration; and *commercial uncertainty*, relating to uncertainty in commercial procurement.

The value estimates given cover the project construction phase, from approval to start of commissioning with beam. They include all the domains of the CLIC complex from injectors to beam dumps, together with the corresponding civil engineering and infrastructures. Items such as specific tooling required for the production of the components, reception tests and pre-conditioning of the components, and commissioning (without beam) of the technical systems, are included. On the other hand, items such as R&D, prototyping and pre-industrialisation costs, acquisition of land and underground rights-of-way, computing, and general laboratory infrastructures and services (e.g. offices, administration, purchasing and human resources management) are excluded. Spare parts are accounted for in the operations budget. The value estimate of procured items excludes VAT, duties and similar charges, taking into account the fiscal exemptions granted to CERN as an Intergovernmental Organisation.

The CLIC value estimates are expressed in Swiss francs (CHF) of December 2018. The breakdown of the resulting cost estimate up to the sub-domain level is presented in Table 3. The injectors for the main beam and drive beam production are among the most expensive parts of the project, together with the main linac, and the civil engineering and services.

Table 3: Cost breakdown for the 380 GeV stage of the CLIC accelerator, for the drive-beam baseline option and for the klystron option.

Domain	Sub-Domain	Cost [MCHF]	
		Drive-beam	Klystron
Main Beam Production	Injectors	175	175
	Damping Rings	309	309
	Beam Transport	409	409
Drive Beam Production	Injectors	584	—
	Frequency Multiplication	379	—
	Beam Transport	76	—
Main Linac Modules	Main Linac Modules	1329	895
	Post Decelerators	37	—
Main Linac RF	Main Linac Xband RF	—	2788
Beam Delivery and Post Collision Lines	Beam Delivery Systems	52	52
	Final focus, Exp. Area	22	22
	Post Collision Lines / Dumps	47	47
Civil Engineering	Civil Engineering	1300	1479
Infrastructure and Services	Electrical Distribution	243	243
	Survey and Alignment	194	147
	Cooling and Ventilation	443	410
	Transport / Installation	38	36
Machine Control, Protection and Safety Systems	Safety System	72	114
	Machine Control Infrastructure	146	131
	Machine Protection	14	8
	Access Safety & Control System	23	23
Total (rounded)		5890	7290

The cost estimate of the initial stage including a 1σ overall uncertainty is:

$$\text{CLIC 380 GeV drive-beam based: } 5890^{+1470}_{-1270}\,\text{MCHF};$$

$$\text{CLIC 380 GeV klystron based: } 7290^{+1800}_{-1540}\,\text{MCHF}.$$

The estimated cost of the initial stage is approximately 5.9 billion CHF. The energy upgrade to 1.5 TeV has an estimated cost of approximately 5.1 billion CHF, including the upgrade of the drive-beam RF power. The cost of the further energy upgrade to 3 TeV has been estimated to be approximately 7.3 billion CHF, including the construction of a second drive-beam complex.

A first estimate of the explicit labour needed for construction of the 380 GeV stage of the CLIC accelerator complex was obtained by scaling with respect to the LHC – a CERN-hosted collider project of similar size to CLIC – yielding 11500 FTE-years of explicit labour. This is in line with the ILC estimate of 1.8 FTE-year/MCHF.

The methodology used for estimating the cost of the CLIC detector [9] is similar to that used for the accelerator complex, and is based on the detector work breakdown structure. A breakdown of the value estimate for the CLIC detector is given in Table 4, and comes to a total of approximately 400 million CHF. The main cost driver is the cost of the silicon sensors for the 40-layer Electromagnetic Calorimeter (ECAL). For example, a 25% reduction in the cost of silicon per unit of surface would reduce the overall detector cost by more than 10%. Alternative designs for ECAL are feasible, but will reduce the detector performance (e.g. worse energy resolution for photons [9]).

Table 4: Cost estimate of the CLIC detector [30].

System	Cost fraction	Cost[MCHF]
Vertex		13
Silicon Tracker		43
Electromagnetic Calorimeter		180
Hadronic Calorimeter		39
Muon System		16
Coil and Yoke		95
Other		11
	0 10% 20% 30% 40% 50%	
Total		397

Operating costs A preliminary estimate of the CLIC accelerator operation cost, including replacement/operation of accelerator hardware parts, RF systems, and cooling, ventilation, electronics, and electrical infrastructures, amounts to 116 MCHF per year.

An important ingredient of the operation cost is the CLIC power consumption and the corresponding energy cost. This is difficult to evaluate in CHF units, as energy prices are likely to evolve. The expected energy consumption of the 380 GeV CLIC accelerator, operating at nominal luminosity, corresponds to 2/3 of CERN's current total energy consumption.

The level of personnel needed for CLIC operational support is expected to be at the level of ILC estimates of 640 FTE.

Given the considerations listed above, one can conclude that operating CLIC is well within the resources deployed for operation at CERN today. Operating CLIC concurrently with other programmes at CERN is also technically possible. This includes LHC, as both accelerator complexes are independent. Building CLIC is not destructive with respect to the existing CERN accelerator complex. Electrical grid connections are also independent. The most significant limitation will therefore be the resources, in particular personnel and overall energy consumption.

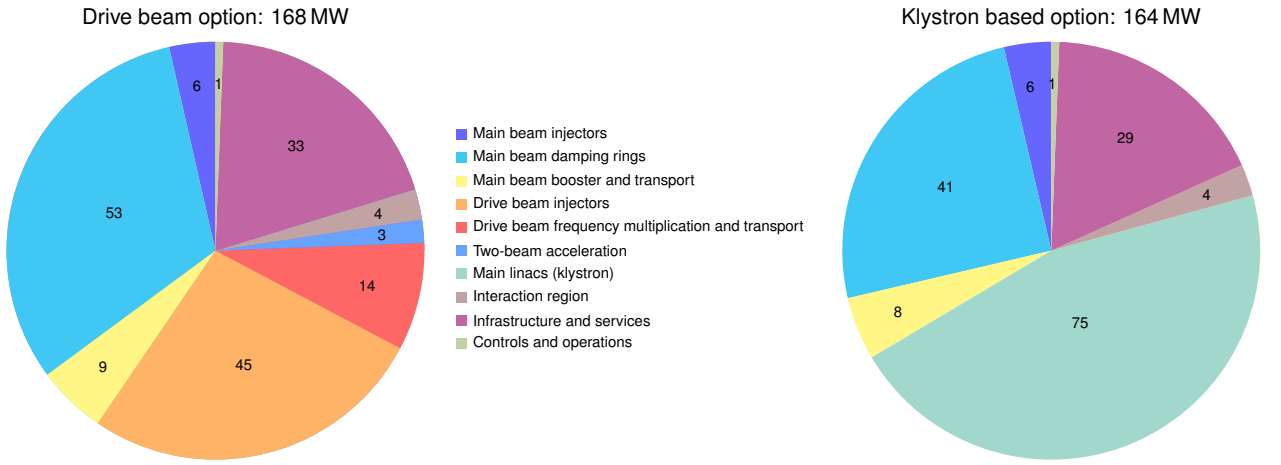


Figure 10: Breakdown of power consumption between different domains of the CLIC accelerator in MW at a centre-of-mass energy of 380 GeV, for the drive beam option on the left and for the klystron option on the right. The contributions add up to a total of 168 MW and 164 MW in the two cases. (image credit: CLIC)

Power and energy consumption The nominal power consumption at the 380 GeV stage has been estimated based on the detailed CLIC work breakdown structure. This yields for the drive-beam option a total of 168 MW for all accelerator systems and services, taking into account network losses for transformation and distribution on site. The breakdown per domain in the CLIC complex (including experimental area and detector) and per technical system is shown in Figure 10.

These numbers are significantly reduced compared to earlier estimates due to optimisation of the injectors for 380 GeV, introducing optimised accelerating structures for this energy stage, significantly improving the RF efficiency, and consistently using the expected operational values instead of the full equipment capacity in the estimates.

The electrical energy consumption estimate is derived from the power consumption described above, and the operational scenario including ramp-up. For the 1.5 TeV and 3.0 TeV stages the recent power improvements have not been studied in detail and the power estimates from the CDR are used [4]. The time evolution of the electrical energy consumption is illustrated in Figure 11. For comparison, CERN's current energy consumption is approximately 1.2 TWh per year, of which the accelerator complex uses approximately 90%.

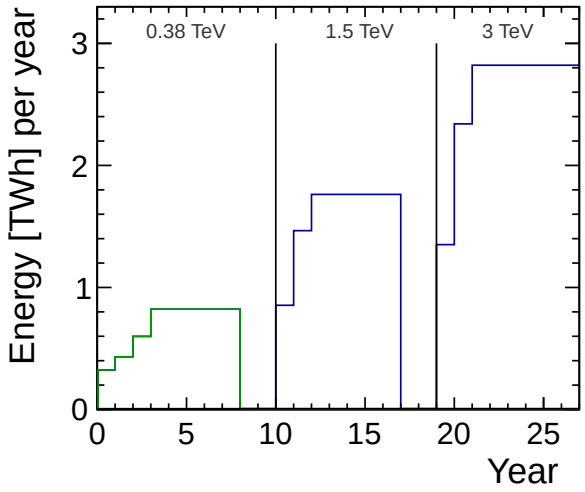


Figure 11: Estimated yearly energy consumption of CLIC. The initial stage estimate is revised in detail (green), while numbers for the higher energy stages are from [4] (blue). (image credit: CLIC)

A.4. Computing

In view of the time scale for the project, no detailed planning of the computing needs for the detector has been established so far. An upper limit of the data volume per train and the data rate written to tape was estimated for the full CLIC detector, including zero suppression and address encoding. The data volume per bunch train ranges from 75 MB at 380 GeV to 115 MB at 3 TeV. With a bunch-train repetition rate of 50 Hz, this results in data rates ranging from $\sim$4 GB/s at 380 GeV to $\sim$6 GB/s at 3 TeV [11]. These numbers are mainly driven by the beam-induced backgrounds.

For comparison, the CMS permanent storage rate is currently at the level of $\sim$5 GB/s, after the trigger and further online data treatment. Therefore, one can conclude that the computing needs for the CLIC experiment will not exceed those of a current multi-purpose LHC detector.